# ANALYSIS OF STRUCTURAL CHANGES DURING EXTENSION IN RING YARN WITH IMAGE PROCESSING SYSTEM

A. KUMAR, S. M. ISHTIAQUE, A. DAS
*Department of Textile Technology, Indian Institute of Technology, New Delhi 110 016, India*

**Abstract**: Changes in internal structure of yarn with extension have been studied using a newly developed and dedicated image processing system and multi colored tracer fibre technique.3D trajectory of whole length of the tracer fibre has been plotted at different extension levels. To assess the structural changes in yarn during extension the cross-section of yarn has been divided into annular concentric rings of equal width. Internal structure parameters like spatial orientation angle, helix angle, migration angle, different cosine angles, twist, and radial packing density in each concentric zone and their average value has been calculated at different extension levels using the images grabbed by the image processing system in two orthogonal planes. Further average changes with yarn extension in fibre extent, actual fibre length and fibre slippage have been quantified. Besides to study the changes in structural parameters with yarn extension along the length of yarn, each fibre has been divided into ten equal segments and above parameters has been quantified in each segment. Special modules of software have been developed in MATLAB to study the above 3D structure parameters of yarn.

**Key words:** Internal structure, 3D trajectory, radial packing density, spatial orientation angle.

## Introduction

Load-extension of staple yarn has been a topic of intense research since the beginning of 20th century. Gegauff [1], Gurney [2], Gregory [3, 4], Bogdan [5, 6] and Iyengar and Gupta [7, 8] have tried to estimate the strength of staple empirically. Hearle *et al.* [9] Zurek [10] and Postle *et al.* [11] have tried to establish fundamental theories for short staple yarn based on fore deformation analysis. Energy approach also been used by Hearle et al. [9] to analyse the tensile behavior of short staple yarn. Langenhove [12] has developed a finite element model to calculate the tensile load and the untwisting moment of yarn at a certain strain, given the structure of the yarn and the properties of its fibers. Still the complete understanding of the mechanism of relationship between tensile extension behaviour of staple yarns and the properties of the constituent fibres on one hand and the detailed structural geometry of the yarn on the other hand has eluded the textile scientist. This is probably because no effort has been made to analyse experimentally the changes taking place in fibres as lying in the yarn and dynamics of internal yarn geometry of yarn on tensile extension. Besides, most of these works are concerned with modulus and strength of yarn and almost no work has been done related to progressive deformation mechanism of staple yarn under extension. Keeping this in view a new image processing system has been designed and developed to measure the changes in internal structure of yarn on extension. Suitable image acquisition software has been developed to extract data relating to yarn boundary and multi-coloured tracer fibres from the images captured at different extension levels.

Further, no studies have been made to assess the changes in internal yarn structure on yarn extension. Hence present study is aimed to assess and quantify with above image processing system, the changes during extension in internal structure parameters like migration, helix angle, spatial orientation angle, migration angle, actual fibre length in the yarn, fibre extent, helix angle and packing density, calculated on the basis of 3D trajectory of the tracer fibre. The phenomenon of fibre untwisting, straightening, straining and slip has also been investigated in detail.

In addition to it, Ishtiaque [13] observed that radial packing density in ring yarn is neither uniform across the yarn cross-section, nor is it maximum at yarn core. Besides Ishtiaque *et al.*

[14] have also observed that yarn packing density is always higher at the middle portion of the fibre in comparison to trailing or leading portion. Hence changes in internal structure of the yarn along the length of the fibre and across yarn cross-section have also been investigated.

## Material and methods

Image processing system consisting of “Microcontroller based 3-D Yarn Structure Analyser”, and data acquisition software designed and developed by Ishtiaque *et al*. [15] is being used as experimental setup for different measurement.

To calculate the radial parameters in the cross-section of yarn is divided into 20 annular concentric cylindrical zones of equal radial width of 0.01 mm each. $(x_i, y_i, z_i)$ co-ordinates are placed in these zones according to their radial position. Thus a set of triplets lying in each zone is obtained. Different internal structure parameters are calculated using these sets of triplets in each zone.

To study the structural changes with yarn extension along the length of fibre each fibre is divided into ten equal segments and structural parameters are calculated for each segment. Front portion of the fibre as coming out from front roller of drafting system of ring frame is considered as leading portion and the back portion as trailing portion. Modules of software have been written in MATLAB7 to calculate different structural parameters.

## Result and Discusion:

### 1. Influence of Extension on Longitudinal Structural Characteristics of Yarn

Many scientists have discussed the slippage phenomenon between fibres in detail. But in no case the fibre slippage in the yarn was quantified. Hence an effort has been made to experimentally measure the increase in fibre length, fibre extent, fibre pair overlap (FPO) and fibre pair index (FPI). FPO and FPI are measured as defined by Ishtiaque *et al.* [16].

The results show an increase in fibre length by 3.05%, 5.32%, and 8.31% when yarn is extended to 4%, 8% and 12% respectively. There is an increase of 3.92%, 6.72% and 9.90% in fibre extent in the yarn on of 4%, 8% and 12% yarn extension respectively. Thus fibre straightening is observed to be 0.87%, 1.40%, 1.59% and slippage is found to be 0.08%, 1.28%, and 2.10% at respective yarn extension percentage. Thus increasing tendency is depicted in matter of straightening and slip on yarn extension. Furthermore there is almost no slip till yarn is extended up to 4%.

FPO value increases as yarn is extended to higher percentage level and observed values are 16.97 mm, 17.66 mm, 18.28 mm and 18.79 mm at 0% 4%, 8% and 12% yarn extension. But no influence on FPI is being noticed due to increase in yarn extension and observed value of FPI is found to be 0.52.

### 2. Impact of Yarn Extension on Twist and Twist Distribution:

Influence of yarn extension on twist and twist distribution is being studied. Twist is being calculated from the triplets of Cartesian co-ordinates obtained from the 3D path of tracer fibre. These Cartesian triplets $(x, y, z)$ are subsequently converted to polar co-ordinates $(r, \Phi, z)$. Two successive polar triplets are considered at a time and using the formula $(t = d\Phi/(dz \times 2 \times \pi))$, proposed by Neckar (2003), twist is calculated at each $z$ value. Average twist of the fibre is calculated by taking the mean of all the values of the twist obtained at each *z* value of all the 40 fibres. To calculate the twist at different radial position, polar triplets are placed in different concentric cylindrical zones as discussed earlier. The process described above is used to calculate the mean value of twist in each zone. Accordingly radial twist distribution in the yarn is obtained. All these calculations are being conceived in special software module written in MATLAB7. To study the variation of twist along the length of fibre all fibres are divided into ten equal segments. It is seen from Figure 1. that average value of twist shows a gradual decreasing trend with increase in yarn extension and the decrease is of the order of 7.82%. The slope of the twist curve is maximum at the 4% to 8% region followed by 0% to 4% and 8% to 12% regions.

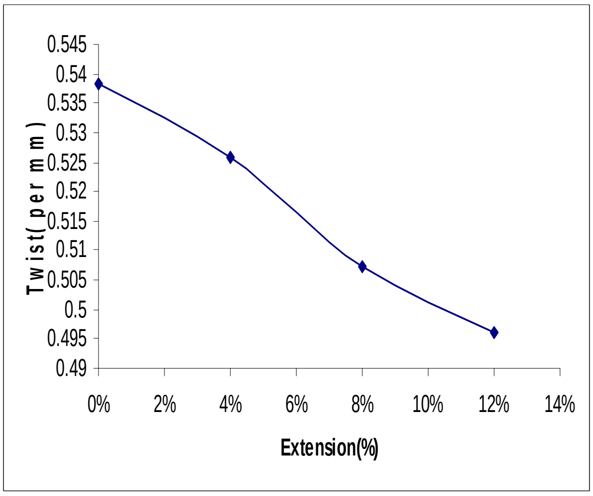


**Figure 1.** Variation of average twist with yarn extension

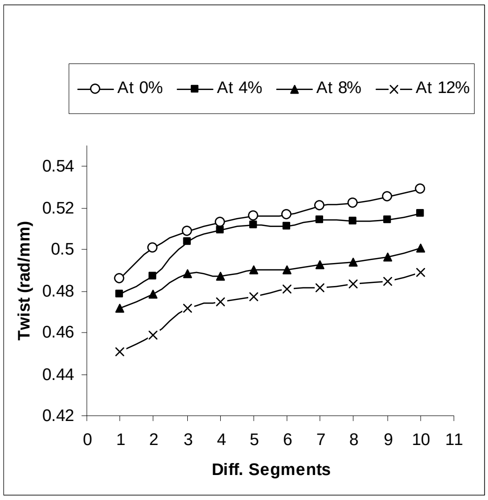


**Figure 2.** Variation of twist with yarn extension in different yarn segments

It is evident from Figure 2 that twist at different percentage of yarn extension along the length of fibres shows an increasing trend from leading to trailing portion. In segments 1 and 2 from the leading side this declining tendency is steeper when yarn is yarn is extended from 8% to 12%. On the other hand this falling gradient is more in segment 3 to 10 when yarn is extended from 4 to 8%. Thus changes are non uniform along the length of the fibres.

It is noticed from Figure 3. that twist at 0% yarn extension increases steeply up to the second zone and thereafter it falls steeply till the 5$^{th}$ zone and in the subsequent zones it remains almost constant. It is further observed that at different percentage of yarn extension twist gradually falls down in second to ninth zone but in subsequent zones no regular trend is noticed.

## 3. Effect of Extension on Packing Density of Yarn

Average yarn packing density is calculated using formula proposed by Ishtiaque [17] Set of polar triplets placed in each cylindrical zone are obtained. Total length of the fibres lying in each zone is calculated. Afterwards the formula proposed by Neckář [18] is applied to determine the packing density in each zone. All these computations are performed in special software module written in MATLAB7. To study the variation of packing density along the length of fibres each fibre is divided into ten segments as discussed earlier and different input variables used by Ishtiaque [17] are taken into consideration.

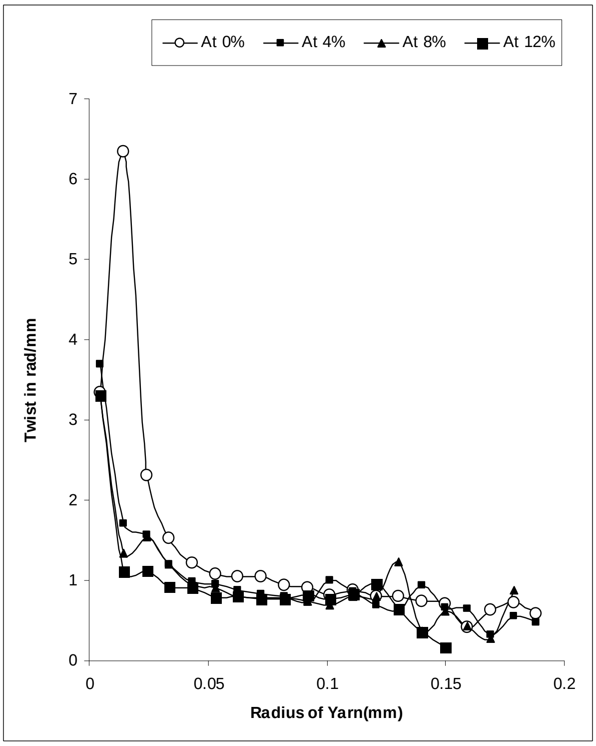


**Figure 3.** Variation of twist in different zones with yarn extension.

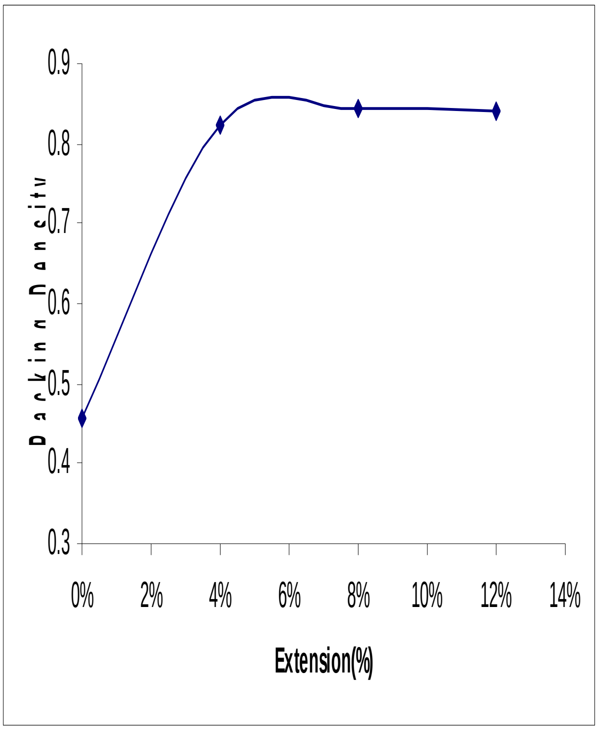


**Figure 4.** Variation of average packing **density with yarn extension**

It has been observed from Figure 4. that for initial 4% extension the increase in average packing density is about 1.8 times. There is very slight increase in packing density on further extension to 8%. It remains almost constant on extension of yarn from 8% to 12%.

It is noticed from the Figure 5, that packing density along the length of fibres at all extension levels shows an increasing trend from leading end to trailing portion.

The study of radial pacing density of yarn at 0% extension from Figure 6. shows that packing density is 0.32 in the 1$^{st}$ zone and it increases to maximum value of 0.67 in the 6$^{th}$ zone corresponding to radial position 0.46 times the radius of yarn. Further it drops sharply up to 16$^{th}$ zone where packing density was found to be 0.01. The results of 4% yarn extension give 0.40 packing density in the 1$^{st}$ zone and maximum packing density of 0.78 in the 5$^{th}$ zone. Thereafter it drops sharply till the 14$^{th}$ zone where 0.01 packing density is attained. In both the cases very low values of packing density are observed in rest of the zones. The radial packing density curve of 8% extension level shows almost similar behaviour as that of 4% extension level. But 0.47 packing density in the first zone, packing density of 0.84 in 5$^{th}$ zone is achieved and 0.008 packing density is found in the 13$^{th}$ zone. Furthermore at 12% yarn extension 0.59 packing density is observed in the 1$^{st}$ zone, attains the maximum packing density of 0.848 in 4$^{th}$ zone and further it declines steeply to attain a value of 0.017 in the 12$^{th}$ zone.

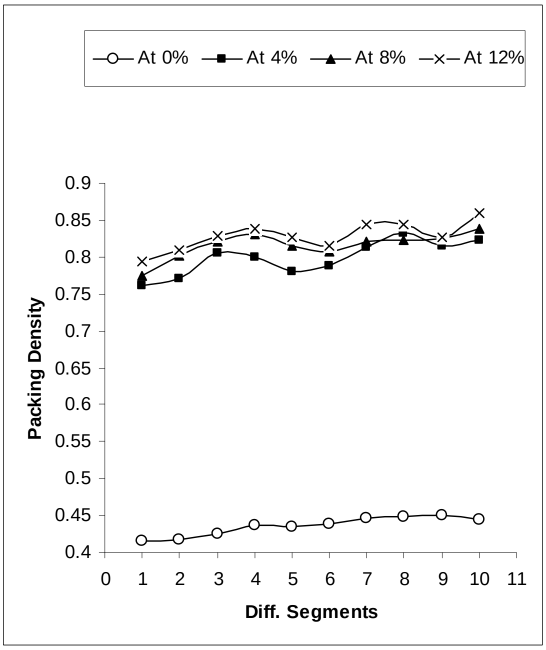


**Figure 5.** Variation of packing density with yarn extension in diff, yarn segments.

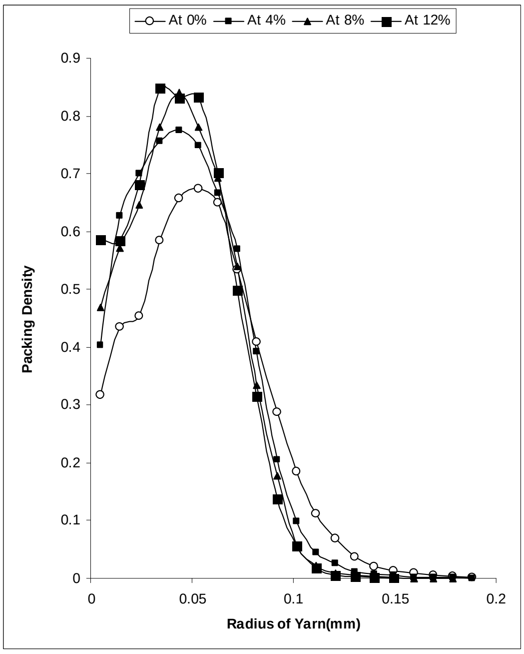


**Figure 6.** Variation of packing density in diff. zones with yarn extension.

On the basis of the above observations it can be concluded that due to yarn extension fibres are pushed to the inner zones of the yarn cross-section. In addition to this it can be noticed that on extension of yarn from 0% to 12% packing density continuously increases in $1^{st}$ zone to $7^{th}$ zone while in $9^{th}$ ring to outer ring a continuous decline of packing density is observed and changes in packing densities in different zones is not uniform across the cross-section of the yarn.

## 4. Impact of Extension on Angular Fibre Orientation

Orientation of the fibres can also be defined in terms of helix angle, migration angle, spatial orientation angle and other related angles. The polar co-ordinates of end points of each elemental fibre segment is considered and different angles are calculated by using the formulae (*β (helix angle)* $=\tan^{-1}(r\times d\Phi/dz)$), (*α(migration angle)* $= \tan^{-1}(dr/dz)$), $\gamma = \tan^{-1}(dr/(r\times d\Phi))$, (*κ(spatial orientation angle)* $= \cos^{-1}(dz/dl)$), $\theta = \cos^{-}1(dr/dl)$ *and* $\chi = \cos^{-1}(r\times d\Phi/dz)$ as proposed by Neckář [19].Weighted means over elemental fibre segments of all the values of angles are calculated . Angles α and β shows radial and twisted migrations respectively and χ is related to orientation of fibres in space with respect to yarn axis. The radial distribution of these angles is calculated by obtaining the mean values of these angles computed for set of polar triplets placed in each zones. Variation of these angles along the length is estimated by dividing the fibres into ten equal segments and calculating these angles separately for each segment. These mathematical operations are being performed in MATLAB7.

It is evident from the Figure 7 and 8 that on yarn extension average radial migration and twisted migration decreases. Besides that on yarn extension fibres are more oriented along the axis of yarn and hence average spatial orientation angle as shown in Figure 9 depicts a decreasing trend on yarn extension. Furthermore, it is observed from the Figure 10 that with yarn extension average $\theta$ remains constant showing that model of equidistant migration as proposed by Neckář [19] holds good at all yarn extension values. Similarly on yarn extension average $\gamma$ also remains constant. On the other hand $\chi$ shows an irregular trend with yarn extension.

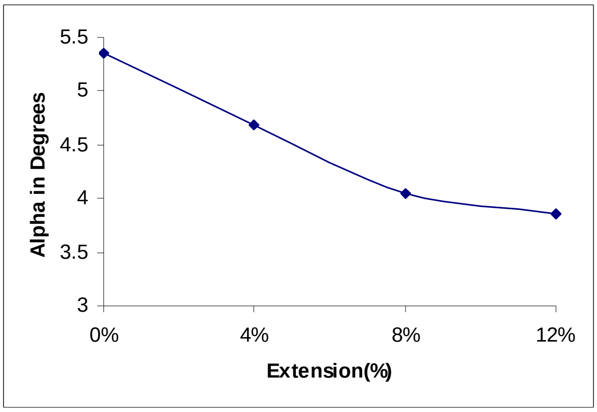


**Figure 7.** Variation of average angle alpha with yarn extension

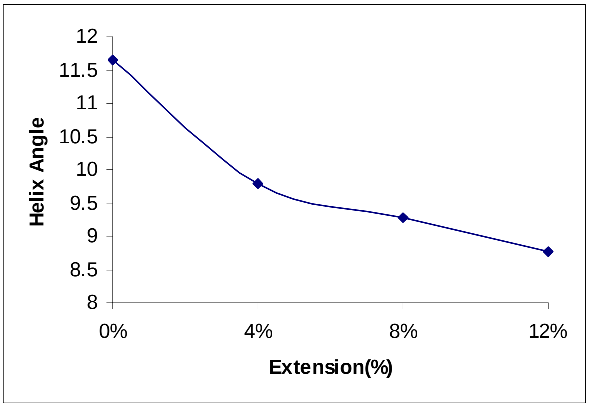


**Figure 8.** Variation of average helix angle with yarn extension

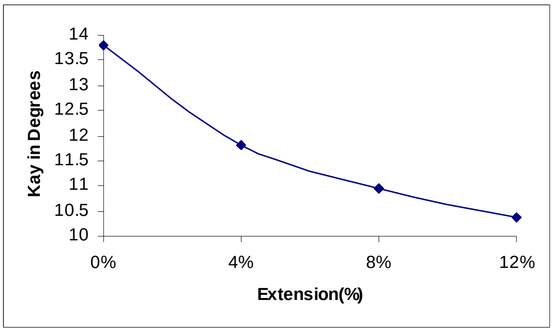


**Figure 9.** Variation of average angle spatial orientation angle with yarn extension

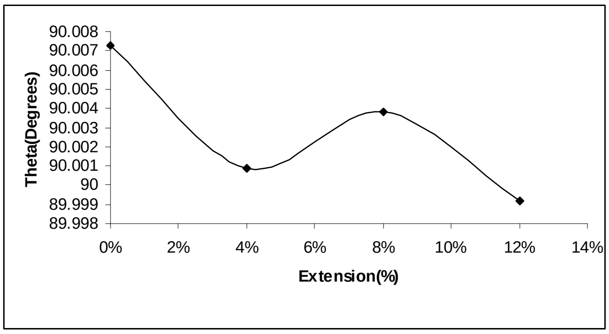


**Figure 10.** Variation of average angle $\theta$ with yarn extension

It can be concluded from Figure 11, 12 that angles $\alpha$, $\beta$ decreases marginally from 1$^{st}$ segment till the 6$^{th}$ segment and then it increases gradually till the 10$^{th}$ segment. Similarly other angles have been studied.

The study of radial distribution of these angles from Figure 13 and 14. brings forth the following conclusions. At 0% yarn extension $\alpha$ falls till the 5$^{th}$ zone, remains unchanged till the 10$^{th}$ zone and shows increasing trend in the subsequent zones. On yarn extension $\alpha$ decreases in the 1$^{st}$ to 9$^{th}$ zone but in the subsequent zones irregular pattern is seen. Helix angle plot at 0% extension remains flat till the 5$^{th}$ zone and afterwards it gradually increases till the 10$^{th}$ zone and beyond this a random pattern is observed. On extending the yarn the helix angle decreases in zones from 2$^{nd}$ to 10$^{th}$ and in rest of the zones an irregular pattern is observed with extension.

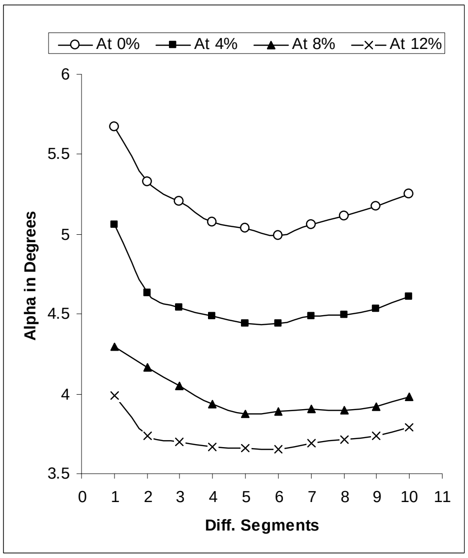


**Figure 11.** Variation of angle alpha with yarn extension in diff. fibre segment

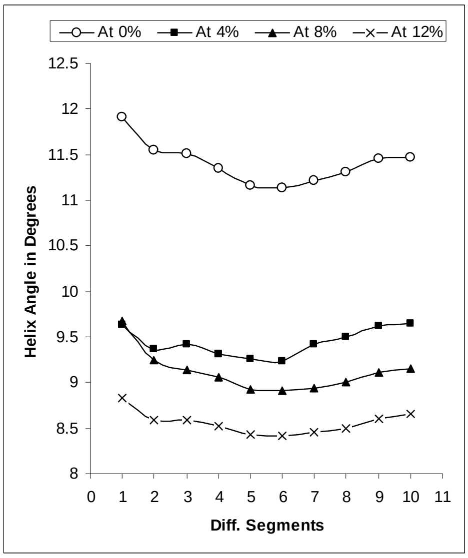


**Figure 12.** Variation of helix angle with yarn extension in diff. fibre segment

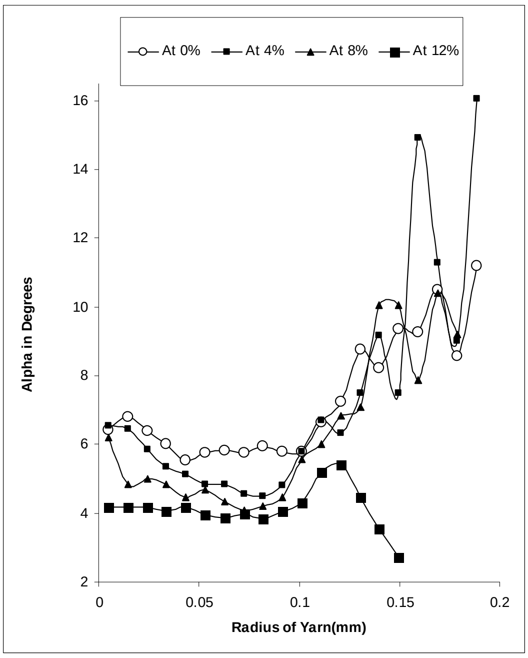


**Figure 13.** Variation of angle alpha in diff. zones with yarn extension.

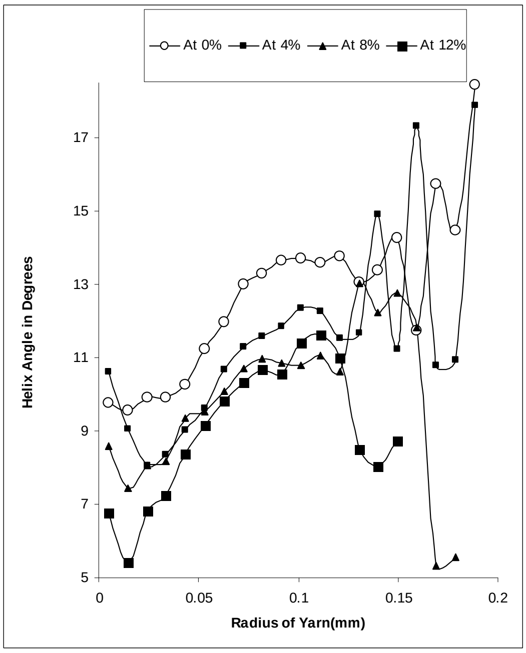


**Figure 14**. Variation of helix in diff. zones with yarn extension.

Almost similar pattern is observed in the case of the spatial orientation angle. Angle θ retains at 90o till the ninth zone at all the extension levels and beyond this zone a random pattern is observed with different percentage of yarn extension. This may tantamount to conclude that model of equidistant migration remains valid till the 9th zone even on yarn extension but in the subsequent zones some amount of deviation is observed with yarn extension. $\gamma$ and $\chi$ show almost similar pattern. Both of these curves, at all extension levels, decreases from 1st to 9th zone and latter an irregular pattern is observed.

**References:**


1 Gegauff, C., 1907, Strength and elasticity of cotton threads, Bulletin *de Societe Industrielle de Mulhouse*, 77, 153-176.
2 Gurney, H. P., 1925, The distribution of stress in cotton products, *J. Text. Inst.*, 16, T269-289.
3 Gregory, J., 1950, Cotton yarn structure, Part III: The strength of artificial yarn elements in relation to bulk and twist, *J. Text. Inst.*, 41, T30-T52.
4 Gregory, J., 1953, Cotton yarn structure, Part V: The relation between strength measurement made on fibres, fibre bundles, yarns and cloth, *J. Text. Inst*., 44, T515-T533.
5 Bogdan, J. E., 1956, The characterization of spinning quality, *Text. Res. J*., 26, 720-730.
6 Bogdan, J. E., 1967, The prediction of cotton yarn strength, *Text. Res. J*., 37,536-537.
7 Iyengar, R. L. N. and Gupta, A. K., 1974a, Proportion of fibre strength utilized in the single yarn, *Text. Res. J*., 44**,** 489-492.
8 Iyengar, R. L. N. and Gupta, A. K., 1974b, Some functions involving fibre properties for estimating yarn tenacity, *Text. Res. J*., 44, 492-494.
9 Hearle, J. W. S., Grosberg, P., and Backer, S., 1969, *Structural Mechanics of Fibres, Yarns and Fabrics*, Wiley-Interscience, New York.
10 Zurek, W., 1975, *The Structure of Yarn*, Foreign Scientific Publications Department of the National Center for Scientific, Technical and Economic Information, Warsaw, Poland.
11 Postle, R., Caranby, G. A. and de Jong, S., 1988, The Mechanics of Wool Structure, *John Willy & Sons, New York.*
12 Langenhove, L. V., 1997, Simulating the mechanical properties of a yarn based on the properties and arrangement of its fibres, Part I: The finite element model,' *Textile Res. J*., 67, 263-268.
13 Ishtiaque S.M., 1986, Radial packing density of rotor- and ring-spun yarns, *Indian J. Text. Res.*, 11, 208-214.
14 Ishtiaque, S. M., Mukhopadhyay, A. and Kumar, A., 2009, Impact of high-speed draw frame and its preparatory on packing and related characteristics of ring spun yarn, *J. Text. Inst.*,100, 657 – 667.
15 Ishtiaque, S.M., Kumar, A., Das A. and Tholeti, P.B., 2010, Development of image processing based system to study yarn structure during extension, *J. Text. Inst*., 101, 687-698.
16 Ishtiaque, S. M., Salhotra, K. R. and Kumar A., 2006, Analysis of spinning process using the taguchi method. Part II: Effect of spinning process variables on fibre extent and fibre overlap in ring, rotor and air-jet yarns, *J. Text. Inst.*, 97, 285-294.
17 Ishtiaque, S.M., 1983, *Selected problems of internal structure of rotor-spun yarn*, Ph.D. thesis, University of Mechanical and Textile Engg., Liberec, Czechoslovakia
18 Neckář, B., 1976, Internal mechanics of twisted yarn, *Text. Res. J*., 46, 545-561.
19 Neckář, B., and Ibrahim, S., 2003, *Structural Theories of Fibrous Assemblies and Yarns*, Technical University of Liberec, Czech Republic.